Performance Evaluation of Fiber-Edge Magnetooptic Probe

Shinichi Wakana, *Member, IEEE,* Etsushi Yamazaki, Shunsuke Mitani, Hyonde Park, Mizuki Iwanami, Shigeki Hoshino, Masato Kishi, and Masahiro Tsuchiya, *Member, IEEE*

***Abstract*—The performance (bandwidth, sensitivity, and spatial resolution) of a fiber edge magnetooptic (FEMO) probe developed for observing three-dimensional magnetic-field distributions was evaluated. A gigahertz bandwidth was achieved without any magnetic bias by using the magnetization rotation in a magnetooptic crystal. The ferromagnetic resonance restricted the observation bandwidth to around 10 GHz. Precise adjustment of the polarization and efficient use of the optical amplifier enhanced the magnetic field sensitivity, enabling an electric current of less than 0.05 mA to be detected. The concept of "sensitive volume" was used to measure the spatial resolution in three-dimensional space; reducing the sensitive volume improved the spatial resolution. Magnetic fields above a microwave patch antenna and around a 10-μm-class circuit board were observed using FEMO probes. The FEMO probe should thus be effective for evaluating microwave and miniature circuits.**

***Index Terms*—Faraday effect, ferromagnetic resonance, magnetic-field distribution, polarization control, rotation magnetization, sensitive volume.**

I. Introduction

THE performance of electronic instruments and devices continues to be enhanced, but at the cost of increasingly complicated design. Consequently, operation inspection and failure analysis have become increasingly difficult. Moreover, analysis techniques often have lower development priority than design techniques, resulting in a lack of sufficient analysis techniques. Particularly difficult is analysis of the electromagnetic field around high-speed electronic circuits in terms of sensitivity and spatial resolution because of their complicated design. Valdmanis and Mourou developed an optical sampling technique based on the electrooptic effect [1] and observed the electric signal at various points in a device under test (DUT) [2]. Several years later, the two-dimensional electric field distribution of a circuit was observed by scanning the electrooptic crystal [3]. Since the electrooptic effect can be used to detect electric field changes of more than 100 GHz with sufficient sensitivity and spatial resolution, the electrooptic sampling technique is suitable for electric field analysis in the microwave range.

In contrast with the electrooptic effect, light interacts with a magnetic field through the magnetooptic (MO) effect, especially through the Faraday effect. A magnetic field sensor that uses the magnetooptic effect is commonly used for monitoring high-voltage power lines [4]. Magnetic field sensors detect changes in the magnetic field by measuring the change in the size of the magnetic domain in the crystal. This size change involves domain wall motion, so it responds rather slowly (up to several tens of megahertz) to a change in the magnetic field. Therefore, application of the magnetooptic effect to high-speed high-density circuit and device analysis is difficult.

It has recently been shown that the magnetooptic effect can be used to detect high-frequency magnetic fields by using rotation magnetization with a suitable magnetic dc bias normal to the probe light axis [5], [6]. Ikekame *et al.* used this technique to observe the waveform of the high-speed driving current in a hard-disk-drive head [7]. Because of the magnetic anisotropy of the magnetooptic crystal, aligning the magnetization easy axis and the probe light axis orthogonal to each other eliminates the magnetic bias. This configuration has been used to detect high-frequency magnetic fields [8], [9]. Its use enables utilization of the high potentiality of light in terms of speed and noninvasiveness for magnetic field observation.

Previous studies demonstrated that a magnetooptic probe should have well-balanced performance in terms of bandwidth, sensitivity, and spatial resolution and led to the development of the fiber edge magnetooptic (FEMO) probe [10].

We have now evaluated the performance of this probe from three viewpoints: bandwidth, sensitivity, and spatial resolution. We have also demonstrated the effectiveness of the probe through two magnetic-field-observation experiments.

II. Configuration of FEMO Probe and Field Observation System

The configuration of the FEMO probe is very simple, as shown in the inset of Fig. 1. A magnetooptic crystal is glued onto a single-mode fiber facet with an ultraviolet curing cement. When the crystal is placed in a magnetic field, the polarization of the laser light circulating through the crystal rotates. The degree of rotation corresponds to the strength of the magnetic field. Note that only the magnetic component parallel to the light axis is measured. The FEMO probe has several advantages compared to the conventional measurement system, which uses discrete optics (i.e., a crystal and lenses). For example, it is

Manuscript received May 5, 2003; revised September 4, 2003. This work was supported in part by Core Research for Evolutional Science and Technology of the Japan Science and Technology Association and the Telecommunication Advancement Organization of Japan.

S. Wakana, E. Yamazaki, S. Mitani, H. Park, and M. Kishi are with the Department of Electronic Engineering, University of Tokyo, 113-8656 Tokyo, Japan.

M. Iwanami and S. Hoshino are with the Association of Super-Advanced Electronics Technologies, 305-0047 Tsukuba, Japan.

M. Tsuchiya was with the Department of Electronic Engineering, University of Tokyo, 113-8656 Tokyo, Japan. He is now with the Communications Research Laboratory, Koganei, Tokyo.

Digital Object Identifier 10.1109/JLT.2003.819794

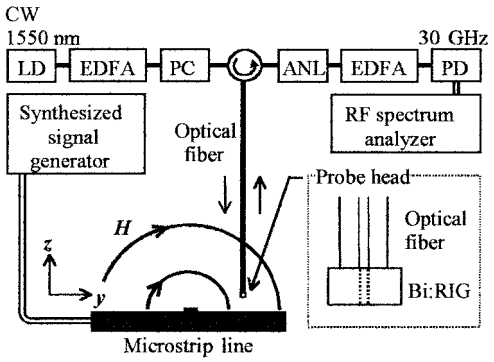

Fig. 1. Configuration of FEMO probe and magnetic-field observation system (LD: laser diode; EDFA: erbium-doped fiber amplifier; PC: polarization controller; ANL: analyzer; PD: photodetector).

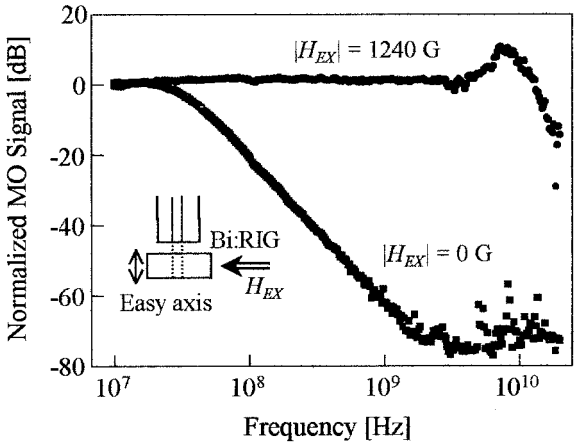

Fig. 2. Frequency response of normalized MO signal with external dc magnetic bias.

robust, so, except for the polarization, the optics do not need to be realigned before use. Furthermore, since it uses a fine crystal and a thin fiber, which have a relatively low dielectric constant, it has low invasiveness and good accessibility to narrow places. In fact, the same design approach could be used to develop a probe for measuring electric fields. The magnetooptic crystal simply needs to be replaced with an electrooptic crystal [11].

The magnetic-field observation system we used to evaluate probe performance is also illustrated in Fig. 1. For the sensing MO crystal, we used commercially available Bi:RIG crystals (Mitsubishi Gas Chemical Ltd.), which were originally developed for the Faraday rotator of optical isolators. A high-reflection (>95%) dielectric multilayered mirror was evaporated on the surface of the crystal opposite to the glued surface. Since Bi:RIG crystals have magnetic anisotropy, the magnetic-field detection performance depends on the arrangement of the optical axis and magnetization easy axis.

The sensing optics consisted of a continuous-wave semiconductor laser, a polarization controller, two optical amplifiers, an analyzer, and a high-speed photodetector. The optical components were connected using an optical fiber. The output signal from the photodetector was evaluated in the frequency domain with a radio-frequency (RF) spectrum analyzer. In contrast with an optical sampling system, which evaluates the signal in the time domain, this system needs neither a pulse laser nor complicated circuitry to synchronize the timing between the DUT driving signal and laser emission. Furthermore, it works as a kind of scalar network analyzer by controlling the operation frequency of the DUT, so the frequency response of the magnetic field of the circuit can be measured easily. As demonstrated previously, the system can be used to acquire the phase information of the magnetic field by replacing the spectrum analyzer with a vector network analyzer [9]. The complete FEMO probing system, including the three-axis motor-driven stage used for scanning the probe head, was controlled with a personal computer.

III. Performance Evaluation

A. Bandwidth

The FEMO probe uses one of two magnetic field detection schemes. First, the relationship between each detection scheme and the bandwidth was examined.

An optical magnetic field sensor based on the Faraday rotation detection scheme generally irradiates the light parallel to the sensor crystal's magnetization easy axis and detects the polarization rotation of the transmitted or reflected light. In this optical configuration, the speed of responding to a change in the magnetic field is restricted by the speed of the magnetic domain wall motion. The domain wall motion is rather slow, so the bandwidth is limited to several tens of megahertz. Consequently, this scheme is not suitable for detecting field changes in the microwave range.

The other scheme is to apply an ac magnetic field orthogonally to the magnetization easy axis. When the ac magnetic field is applied, the magnetization in the crystal starts to rotate. Since this magnetization responds quickly to the high-speed magnetic signal, the bandwidth is wider than that of the first scheme. The arrangement of the optical axis and crystal axes should not be parallel in this detection scheme. The principle of magnetic field detection using rotation magnetization was previously reported [8], [9].

The detection bandwidths with these two schemes were experimentally compared. The magnetization easy axis of the crystal was made parallel to the optical axis, and magnetic dc bias (H_{EX}) was applied normal to these axes. Without the dc bias, the magnetic field could be detected through the domain wall motion (i.e., slow detection method). In contrast, the magnetization inclined with the dc bias field strength, so the rotation magnetization can be used to detect the magnetic field parallel to the optical axis. As shown in Fig. 2, the bandwidth of the rotation magnetization detection scheme exceeded 10 GHz, and the response was almost flat up to about 8 GHz under a certain bias condition. The resonant peak at 10 GHz was due to the ferromagnetic resonance of the crystal. In contrast, the bandwidth of the domain wall motion detection scheme was less than 20 MHz. The detection bandwidth of the rotation magnetization detection scheme is thus significantly wider. We determined that the detection bandwidth of our magnetic crystal exceeded 5 GHz.

Based on these findings, we fabricated an FEMO probe that uses rotation magnetization detection. First, a thin crystal plate whose magnetization easy axis was in plane was sliced from

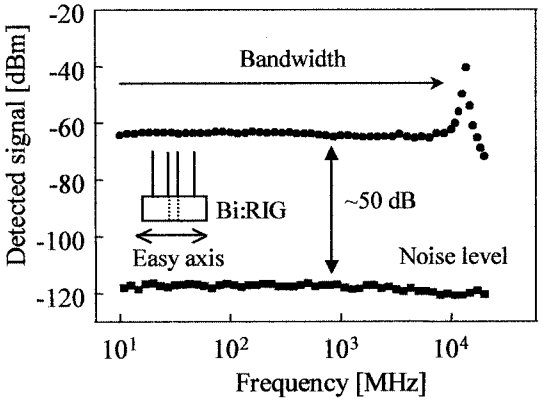

Fig. 3. Frequency response of signal strength and noise level of rotation-magnetization-type FEMO probe.

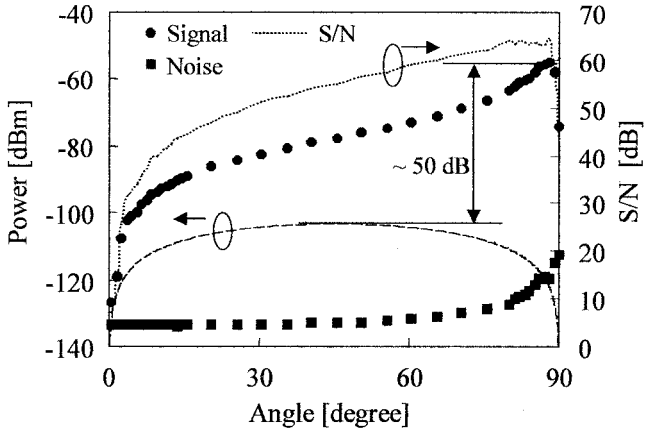

Fig. 4. Analyzer angle dependence of signal strength (black circles: measured signal strength; black squares: measured noise level; dotted line: signal/noise ratio calculated from measured strength; broken line: estimated signal strength calculated without optical amplifier).

a commercial crystal plate whose magnetization easy axis was directed out-of-plane. After polishing of the plate's surfaces, a dielectric mirror was evaporated on one of its surfaces. Because the crystal has a finite refractive index, the FEMO probe works as a magnetic sensor even without a mirror, although at a sacrifice in sensitivity. Finally, the size and shape of the crystal plate were adjusted with a razor blade under a microscope, and it was glued onto a fiber facet. This procedure was designed specifically to reduce the size of the probe head as much as possible, thereby enabling access to confined places.

The frequency response of the signal and the noise level of the rotation magnetization probe are shown in Fig. 3. The DUT was a simple microstrip line, and constant power was supplied from a signal generator. The distance between the crystal's bottom surface and the microstrip line was 20 μm. The response was flat ($\pm$2 dB) up to about 10 GHz.

These results clearly show that the ferromagnetic resonance restricts the detection bandwidth. As previously mentioned, the Bi:RIG crystal we used was developed for the Faraday rotator of optical isolators, so its composition was not optimized for magnetic sensors. Careful control of the composition of the ferrite crystals should increase their ferromagnetic resonant frequency [12], [13]. In fact, a magnetooptic detection bandwidth of 80 GHz has been experimentally obtained using a special crystal [14]. An even wider bandwidth and enhanced optical performance (lower loss and a higher Faraday rotation angle per unit field strength) are desired for future magnetooptic crystal development.

B. Sensitivity

The signal-to-noise ratio of the FEMO probe was estimated to be 50 dB based on the results shown in Fig. 3. Since an RF power of 20 dBm was applied to the microstrip line, the minimum detectable power level was -30 dBm. This corresponds to a current sensitivity of about 140 μArms with 50-Ω circuit impedance. The detectable magnetic field sensitivity was calculated to be about 1 A/m (14 mOe) at the bottom surface of the crystal. Considering the nonuniformity of the field in the crystal, this seems to be the worst case; however, this sensitivity is still about one order of magnitude higher than that of conventional magnetooptic magnetic field sensors [15].

This higher sensitivity is due to the special detection optics of the FEMO probe system, in particular, the effective use of the optical amplifiers and the optimization of the analyzer angle. In the arrangement we used (Fig. 1), the light incident to the crystal and the light transmitted to the analyzer are separately amplified to specific levels with two separate fiber amplifiers. There is thus no shortage of light power as there often is in optical measurement systems.

The analyzer angle was optimized using another experiment. As illustrated in Fig. 4, the origin of the analyzer angle (0°) was first determined by searching for the minimum-output power angle (90°) without applying a magnetic field. The output polarization state of the polarization controller was also optimized in this step. As a result, the light incident to the analyzer was linearly polarized, and its angle was 0°. Then, the analyzer angle dependencies of the signal strength and the noise level were measured. The signal strength gradually increased as the analyzer angle was increased; it reached a maximum at around 88° and then suddenly decreased. The noise level remained constant up to around 60°, then increased. A very high current sensitivity of about 0.8 μArms was obtained at an angle of 88°; this sensitivity corresponds to a magnetic field sensitivity of 0.2 A/m (2.8 mOe). The dashed line in Fig. 4 shows the calculated angle dependence of the signal strength assuming no second amplifier and that the first amplifier compensates for all the loss in optical power. In this case, the maximum signal strength was obtained at 45°. The tendencies are quite different, and the signal-level difference is about 50 dB, which is very difficult to compensate for with an electronic amplifier. This suggests that the FEMO probe system does not simply detect the optically amplified output from the analyzer.

We investigated the origin of the probe's high sensitivity by considering the power and polarization changes of the probe light. The changes in the carrier and signal light in the frequency domain are schematically shown in Fig. 5(a)–(c). They were measured immediately after the light was output from the crystal, the analyzer, and second amplifier, respectively. Since the crystal was thin and the magnetic field was weak, the rotation angle was less than 0.1°, and the power of the signal compo-

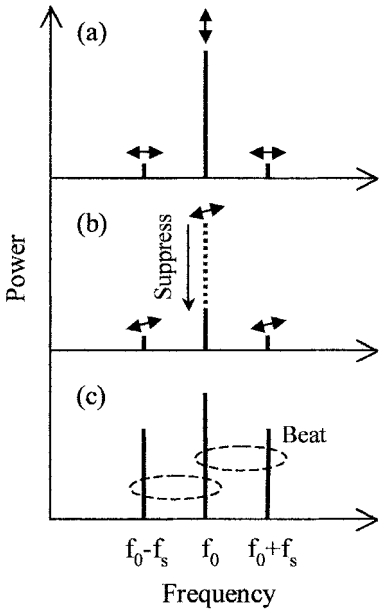

Fig. 5. Schematic image of power change of carrier and signal lights in frequency domain: (a) output from crystal, (b) output from analyzer, and (c) output from second amplifier. Note that the vertical axis does not reflect exact signal strength.

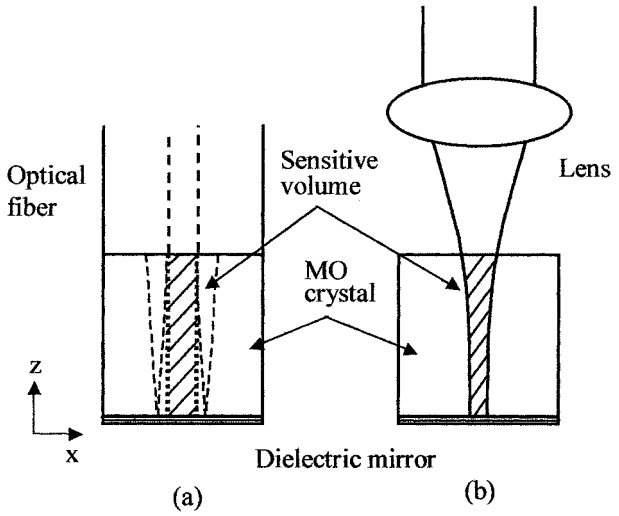

Fig. 6. Sensitive volumes in crystals: (a) FEMO probe case and (b) space optics case.

nent was less than 0.1% (−30 dB) that of the carrier component [Fig. 5(a)]. When the analyzer angle was set almost orthogonal to the polarization direction of the carrier, most of the carrier component was suppressed [Fig. 5(b)]. The second optical amplifier then amplified both the suppressed carrier and the weak signal [Fig. 5(c)]. Then, the signal output from the photodetector was modulated with the frequency difference between the carrier and the signal, i.e., the applied field frequency. Finally, the spectrum analyzer detected the power of this beat signal. When the analyzer angle was rather low, the carrier was not sufficiently suppressed, the gain saturated in the second optical amplifier, and the signal component was not sufficiently amplified. Furthermore, if the analyzer angle is set perfectly orthogonal to the polarization direction of the carrier, the beat signal obviously cannot exist without a carrier component. Thus, the high sensitivity of the FEMO system apparently originates in the beat detection scheme and the effective use of the optical amplifier gain to suppress the strong carrier component. The noise component was also analyzed in the same manner and found to consist of amplified spontaneous emission (ASE) noise from the second amplifier, beat noise between the ASE and carrier, and beat noise between the ASE components [16].

We estimate the ultimate current sensitivity limit of the present configuration to be about 10 μArms. Placing narrow-bandwidth optical filters immediately after both amplifiers would reduce the ASE components of their outputs, which would suppress the noise level and prevent the gain saturation caused by the ASE components. This would enhance the sensitivity.

Although the rotation-magnetization-type FEMO probe has high sensitivity, as shown above, the domain-wall-motion detection-type FEMO probe has even higher sensitivity [17], apparently due to the difference in the Faraday rotation coefficient for unit field strength.

C. Spatial Resolution

Generally, the spatial resolution of an optical probing technique is defined as the spot size of the light at the bottom of the crystal. Since the crystal is directly attached to an optical fiber facet in the FEMO configuration, it is impossible to focus the light onto the crystal bottom surface. The light output from the fiber has a diffraction angle, so the spot size is larger than the diameter of the fiber core. Thus, the spatial resolution of the FEMO probe is worse than the fiber core size based on the conventional definition.

We feel, however, that the conventional definition of spatial resolution is not sufficient when observing a field distribution. First, the crystal and the structure supporting the crystal affect the impedance of the DUT [18]. Second, the electromagnetic field distribution is distorted by the finite dielectric constants of the crystal and by the structures and magnetic permeability of the crystal. Third, the standard definition does not work for a three-dimensional electromagnetic distribution. When observing the field distribution, especially near the DUT, the field transformation in the direction parallel to the optical axis cannot be neglected because the light interacts with this transforming field along the optical path in the crystal. Thus, all of the field information is accumulated in the detected signal. Imagine a thick crystal in a field that varies three-dimensionally. Information from the bottom area of the crystal reflects the sharp variations in the field, while information from the top area reflects a rather slow field, resulting in a rather hazy observed distribution. The traditional definition fails in such circumstances.

The concept of "sensitive volume" can be used to solve the definition problem [19]. It refers to the volume of the area in which a light interacts with a field in a crystal. In the FEMO probe, only the light is reflected back to the core. It reenters the core and contributes to the detection, even though the spot size expands due to the diffraction. Therefore, the sensitive volume of the FEMO probe is like a column, as shown by the hatched area in Fig. 6(a). Its diameter is equal to the diameter of the fiber core, and its height is equal to the thickness of the crystal.

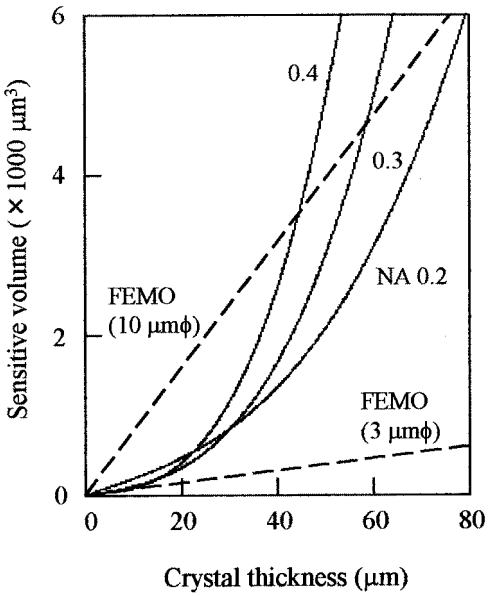

Fig. 7. Relationship between crystal thickness and sensitive volume. Two broken straight lines are for FEMO probe having mode field diameter of 3 or 10 μm. Three solid lines are for conventional space optics (focusing lens has numerical aperture of 0.2, 0.3, or 0.4). Refractive index of crystal was assumed to be 2.2.

Note that the diameter is independent of the crystal thickness. In contrast, the sensitive volume with conventional space optics depends on the crystal thickness, the refractive index of the crystal, and the numerical aperture of the lens, as illustrated in Fig. 6(b).

Fig. 7 shows the dependence of the sensitive volume on crystal thickness. The refractive index of the crystal was assumed to be 2.2 [20]–[22]. Since the crystal needs to be at least 20–30 μm thick to enable it to be processed and handled, the sensitive volume of the FEMO probe is not very large. A probe with an even smaller sensitive volume could be fabricated by using a narrower core (e.g., 3 μm) fiber, although this would sacrifice optical power efficiency. For spatial distribution observation, the spatial resolution apparently has a close relationship with the sensitive volume.

The concept of sensitive volume can also be used to evaluate the degree of the spatial resolution of the FEMO probe compared with the required resolution. The detailed evaluation procedure is described using the following example.

First, the two-dimensional dc magnetic field distribution under consideration [Fig. 8(a)] is calculated in 5-μm steps using Biot–Savart's law. In this example, currents on three parallel transmission lines generate the magnetic field. The calculation step does not need to be very precise. The lines are 50 μm wide and 150 μm apart. The direction of each current is normal to the surface, and the amount of the currents is the same. Since the aim of this calculation is a rough estimation of the magnetic field distribution, the amount of the current does not need to be quantitative.

Next, the two-dimensional Fourier spectrum of the calculated field distribution [the first quadrant of which is shown in Fig. 8(b)] is calculated. As shown in Fig. 8(b), the high spatial

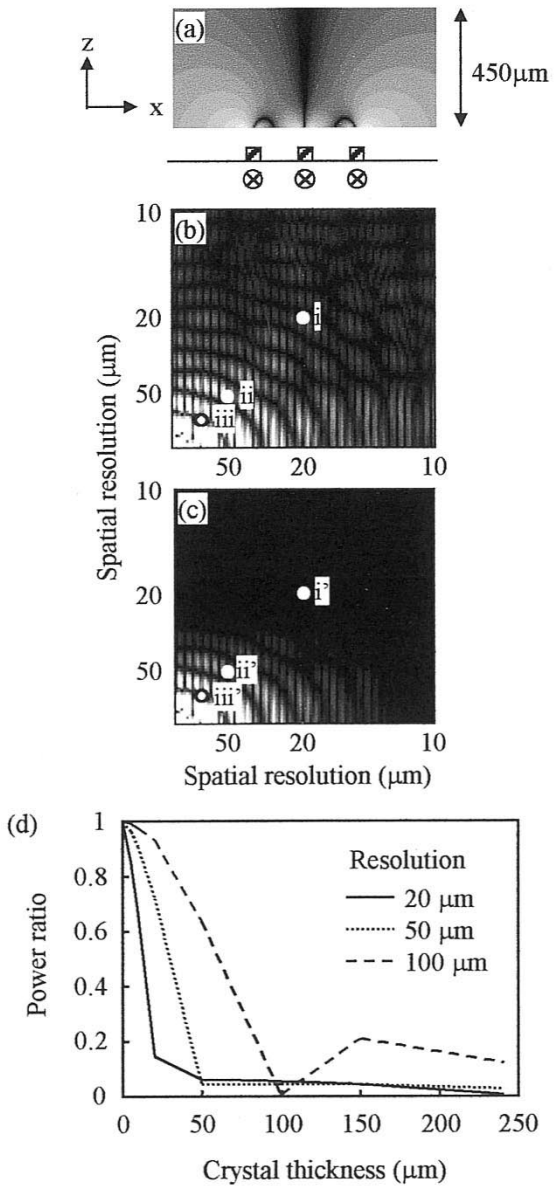

Fig. 8. Results of spatial resolution estimation of FEMO probe: (a) calculated magnetic field distribution in x-z plane under observation (z-component), (b) two-dimensional power distribution of Fourier transformation of calculated field, (c) filtered power distribution of field, which emulates degradation in observed field distribution (20-μm-thick crystal probe was assumed for calculation of filter pattern), and (d) relationship between crystal thickness and power conservation ratio at specific spectrum points. Solid, dotted, and broken lines show dependence at test points of 20 × 20, 50 × 50, and 100 ×100 μm, respectively.

frequency component is contained in the magnetic field. In other words, the figure shows the spatial frequency bandwidth needed for observing the field accurately.

Then, the two-dimensional Fourier spectrum of the sensitive volume is calculated and applied to the previously estimated spatial spectrum. The sensitive volume is treated as a rectangular spatial filter (i.e., a low-pass filter in the spectral domain) in this step. This filtering operation corresponds to field distribution observation using the FEMO probe. Fig. 8(c) shows the Fourier spectrum after applying the spatial filter (assuming a sensitive volume of 10×20 μm).

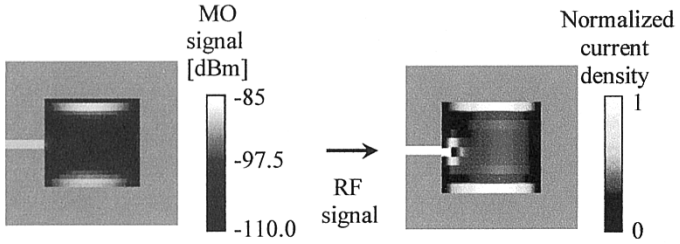

Fig. 9. Magnetic field distribution of microwave patch antenna: (a) observed z-component magnetic field distribution above antenna and (b) current distribution on antenna simulated using Sonnet-Lite [23].

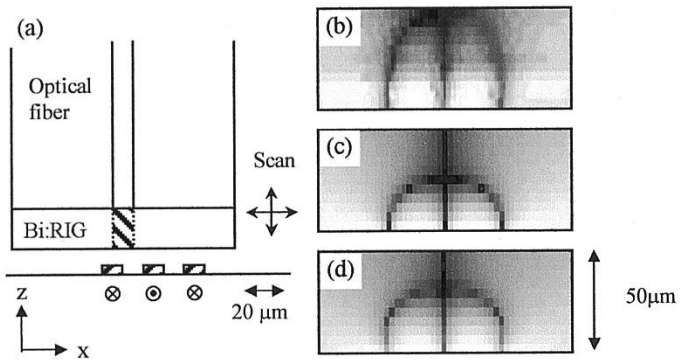

Fig. 10. Magnetic field distribution of 10-μm-class circuit: (a) schematic layout of FEMO probe and printed circuit, (b) observed magnetic field distribution, (c) field distribution calculated using Biot–Savart's law without considering magnetic permeability of crystal, and (d) field distribution calculated using FEM magnetics and considering anisotropic permeability of crystal.

Next, the power conservation ratio between before and after filtering is calculated at three points in the spectrum. These points are indicated in Fig. 8(b) and (c) as i), ii), iii) and i′), ii′), iii′). They correspond to spatial resolutions of 20 $\times$ 20, 50 $\times$ 50, and 100 $\times$100 μm, respectively. We refer to the power at these points as Pi and Pi′; Pi′/Pi represents the power conservation ratio after filtering. Fig. 8(d) shows the dependence of the power conservation ratio on the crystal thickness. The sensitive volume diameter was fixed at 10 μm in this calculation. The thinner crystals clearly conserve higher spatial frequency components. For example, a 20-μm-thick crystal conserves a spectral component of 20 $\times$20 μm, while a 100-μm-thick crystal almost loses even a 100 $\times$100 μm component.

The magnetic field distribution under consideration has components less than 20 $\times$20 μm [from Fig. 8(b)]. Thus, the crystal thickness needs to be less than at least 20 μm [from Fig. 8(d)] to observe the field with an adequate resolution. This is a typical example of crystal size design, and it shows the effectiveness of using the concept of sensitive volume. This procedure could also be used to optimize the sensitive volume for a specific purpose.

To achieve the required spatial resolution, an appropriate fiber core size and crystal thickness must be selected. The smaller the core, the better the resolution, though selection of the core size is limited. The dependence on crystal thickness differs between spatial resolution and magnetic field sensitivity. The thinner the crystal, the better the resolution; however, the shorter the interaction length, the weaker the output signal. Therefore, the crystal should be as thick as possible to obtain the required spatial resolution and sufficient sensitivity.

In summary, the spatial resolution of an optical probing system is restricted by its sensitive volume. The resolution and sensitivity of the FEMO probe can be optimized by analyzing the spatial frequency spectrum of both the field distribution and the sensitive volume.

IV. Experimental Demonstration

We conducted two experiments to demonstrate the performances of the FEMO probe. In the first, we observed the magnetic field distribution above a microwave patch antenna in the x-y plane. In the second, we observed the field around the fine wires in the x-z plane.

In the first experiment, a 6.7-GHz 20-dBm sinusoidal signal was supplied to a 10-mm^2 patch antenna. Using an electrooptic sampling technique [23], Yang *et al.* were able to observe the electric near field above an antenna, but rarely the magnetic one. Using the FEMO probe, we were able to observe the magnetic near-field 50 μm above the antenna. Fig. 9(a) shows the observed distribution, and Fig. 9(b) shows the current distribution simulated using finite-element method (FEM) software [24]. The patch antenna has a conductor electrode and a larger grounded electrode. The current forms a standing wave on the conductor electrode in the x-direction at the resonant frequency. The nodes of the standing wave are located at the two vertical edges, while the current concentrates at the two horizontal edges, as shown in Fig. 9(b). There is a magnetic field between the electrodes oriented in the y-direction. There is a leakage magnetic field with a component perpendicular to the electrode around the horizontal edges. The FEMO probe detects this field, as shown in Fig. 9(a). This observed distribution seems reasonable. The FEMO probe is thus well suited for evaluating microwave devices.

The sample for the second experiment was a meander-type printed Al circuit. The wires were 10 μm wide and 10 μm apart. Fig. 10(a) shows the layout of the probe and the wires. The probe had a 20-μm-thick crystal and was scanned in the plane normal to the wires. The observed magnetic field distribution is shown in Fig. 10(b) [25]; note that the observed field was only the z-component. The field distribution calculated using Biot–Savart's law is shown in Fig. 10(c) for comparison. The laser intensity profile was assumed to be Gaussian, and the product of the laser intensity and the magnetic field strength was integrated along the optical path. The close similarity between those distributions shown in Fig. 10(b) and (c) demonstrate that the FEMO probe can be used to observe the magnetic near field of a 10-μm-class circuit.

The slight distortion of the observed distribution in the z-direction may have been due to the magnetic anisotropic permeability of the MO crystal. The Bi:RIG crystal has magnetic permeability of around 40–100 [26], and the field distribution might have been affected by the presence of the crystal. We estimated this effect using FEM software.[1] As shown in Fig. 10(d), the field distribution was clearly distorted in the z-direction.

[1]http://femm.foster-miller.net/index.html

While this supports our assumption, we cannot completely explain the difference yet.

As shown in Fig. 10(b) and (c), the contributions from each wire in such a fine circuit are indistinguishable at 50 μm. Consequently, the field transition must be precisely observed from the near to far region to identify an electromagnetic interference source in high-density printed circuit boards. The FEMO probe is well suited for such observation.

We are developing a probe with both a wider bandwidth and higher spatial resolution and will present the results elsewhere.

V. Conclusion

The FEMO probe system was experimentally demonstrated to be well suited for observing high-frequency magnetic field distributions (e.g., >10-GHz bandwidth). It has around 20-μA current sensitivity and 10-μm-class spatial resolution. The detection bandwidth was greatly expanded, compared with that of the conventional magnetic domain wall motion detection scheme, by using the rotation magnetization in the magnetooptic crystal. Precise tuning of the crystal composition should result in an even wider bandwidth. The FEMO probe is thus well suited for analysis and design verification of microwave devices and circuits.

Optimization of the polarization and effective use of the optical amplifiers resulted in sensitivity better than that of a conventional Faraday rotation detection sensor. Modification of the detection optics should further improve sensitivity.

Finally, reducing the sensitive volume by using a thinner probe crystal improved the three-dimensional spatial resolution. Using an optical fiber with a narrower core should result in even higher spatial resolution.

The probe best suited for a particular purpose can be selected based on the clarified procedure for designing an FEMO probe. Since the probe head is simple and compact, the probe can access confined places, making it suitable for analyzing high-density circuits, such as assembled printed circuit boards.

In short, the FEMO probe system has well-balanced performance in terms of bandwidth, sensitivity, and spatial resolution. It is thus an effective magnetic field observation system for electronic circuit analysis.

References

[1] J. A. Valdmanis and G. A. Mourou, "Subpicoecond electrical sampling and applications," in *Picosecond Optoelectronic Devices*. New York: Academic, 1984, pp. 249–270.

[2] J. A. Valdmanis and S. S. Pei, "A noncontact electro-optic prober for high speed integrated circuits," in *Picosecond Electronics and Optoelectronics II*. Berlin, Germany: Springer-Verlag, 1987, pp. 4–10.

[3] *1994 IEEE MTT-S Int. Microwave Symp. Dig.*, vol. 3, 1994, pp. 1597–1600.

[4] Y. N. Ning, Z. P. Wang, A. W. Palmer, K. T. V. Grattan, and D. A. Jackson, "Recent progress in optical current sensing techniques," *Rev. Sci. Instrum.*, vol. 66, pp. 3097–3111, 1995.

[5] M. R. Freeman, "Picosecond pulsed-field probes of magnetic systems," *J. Appl. Phys.*, vol. 75, pp. 6194–6198, 1994.

[6] E. Yamazaki, S. Wakana, M. Kishi, and M. Tsuchiya, "10 GHz-class magneto-optic field sensing with bi-substituted rare-earth ion garnet rotation magnetization employed," *Jpn. J. Appl. Phys.*, vol. 41, pp. 904–907, 2002.

[7] H. Ikekame, K. Nakamoto, N. Nishiyama, T. Tsuyoshi, and H. Aoi, "In-situ magnetooptical probing for high-frequency current in magnetic head," in *Dig. 26th Annu. Conf. Magnetics Japan*, vol. 26, 2002, p. 262.

[8] E. Yamazaki, H. Park, S. Wakana, M. Kishi, and M. Tsuchiya, "Implementation of magneto-optic probe with >10 GHz bandwidth," *Jpn. J. Appl. Phys.*, vol. 41, pp. L864–L866, 2002.

[9] E. Yamazaki, S. Wakana, H. Park, M. Kishi, and M. Tsuchiya, "High frequency magneto-optic probe based on BiRIG rotation magnetization," *IEICE Trans. Electron.*, to be published.

[10] S. Wakana, T. Ohara, M. Abe, E. Yamazaki, M. Kishi, and M. Tsuchiya, "Fiber-edge electrooptic/magnetooptic probe for spectral domain analysis of electromagnetic field," *IEEE Trans. Microwave Theory Tech.*, vol. 48, pp. 2611–2616, 2000.

[11] T. Ohara, M. Abe, S. Wakana, M. Kishi, M. Tsuchiya, and S. Kawasaki, "Two-dimensional field mapping of microstrip lines with a band pass filter or a photonic bandgap structure by fiber-optic EO spectrum analysis system," in *Tech. Dig. Int. Topical Meeting Microwave Photonics*, Oxford, 2000, WE2.17, pp. 210–213.

[12] R. Karim, K. D. Mckinstry, J. R. Trudson, and C. E. Patton, "Frequency dependence of the FMR linewidth in single crystal barium ferrite platelets," *IEEE Trans. Magn.*, vol. 28, pp. 3225–3227, 1992.

[13] Y. Iijima, Y. Houjou, and R. Sato, "Millimeter wave absorber using M-type hexagonal ferrite," in *Int. Symp. Electromagnetic Compatibility*, Washington,, DC, 2000, pp. 547–549.

[14] A. Y. Elezzabi, private communication, Nov. 2001.

[15] J. E. Lenz, "A review of magnetic sensors," *Proc. IEEE*, vol. 78, pp. 973–989, 1990.

[16] S. Mitani, E. Yamazaki, M. Kishi, and M. Tsuchiya, "Sensitivity enhancement by optical pre-amplification combined with bias optimization in fiber-optical probing systems for electromagnetic field measurements," in *4th Korea-Japan Joint Workshop Microwave and Millimeter-Wave Photonics P-14*, Daejon, Korea, 2003.

[17] E. Yamazaki, "10 GHz-class magneto-optic probe," Master's thesis, Univ. of Tokyo, Tokyo, Japan, 2002.

[18] T. Nagatsuma, T. Shibata, E. Sano, and A. Iwata, "Subpicosecond sampling using a noncontact electro-optic probe," *J. Appl. Phys.*, vol. 66, pp. 4001–4009, 1989.

[19] S. Wakana, E. Yamazaki, M. Iwanami, S. Hoshino, M. Kishi, and M. Tsuchiya, "Study of a crystal size effect on spatial resolution in three-dimensional measurement of fine electromagnetic field distribution by optical probing," *Jpn. J. Appl. Phys.*, to be published.

[20] J. Gouzerh and A. A. Stashkevlch, "Influence of laser annealing on the index of refraction of a Bi, Ga-doped garnet film," *J. Appl. Phys.*, vol. 69, pp. 5975–5977, 1991.

[21] T. Izuhara, J. Fujita, M. Levy, and R. M. Osgood, "Integration of magnetooptical waveguides onto a III-V semiconductor surface," *IEEE Photon. Technol. Lett.*, vol. 14, pp. 167–169, 2002.

[22] R. Wolfe, J. Hegarty, L. C. Luther, and D. L. Wood, "Single mode magneto-optic waveguide film," *Appl. Phys. Lett.*, vol. 48, pp. 508–510, 1986.

[23] K. Yang, G. David, J. G. Yook, I. Papapolymerou, L. P. B. Katehi, and J. F. Whitaker, "Electrooptic mapping and finite element modeling of the near-field pattern of a microstrip patch antenna," *IEEE Trans. Microwave Theory Tech.*, vol. 48, pp. 288–294, 2000.

[24] Sonnet lite, Sonnet Software Inc..*http://www.sonnetusa.com* [Online]

[25] E. Yamazaki, S. Wakana, M. Kishi, and M. Tsuchiya, "Three-dimensional magneto-optic near field mapping over 10–50 μm-scale line and space circuit patterns," in *14th Annu. Meeting IEEE Lasers Electro-Optics Society (LEOS 2001)*, San Diego, CA, Nov. 2001, TuW6, pp. 318–319.

[26] B. Stadler, K. Vaccaro, P. Yip, J. Lorenzo, Y. Q. Li, and M. Cherif, "Integration of magneto-optical garnet films by metal-organic chemical vapor deposition," *IEEE Trans. Magn.*, vol. 38, pp. 1564–1567, 2002.

Shinichi Wakana (M'92) was born in Tokyo, Japan, on March 13, 1959. He received the B.E. and M.E. degrees in electrical engineering from Waseda University, Tokyo, Japan, in 1982 and 1984, respectively.

He joined Fujitsu Laboratories Ltd., Atsugi, Japan, in 1984. He was a Visiting Scholar at the University of Michigan, Ann Arbor, from 1991 to 1993. He has been engaged in research and development of optical sensing technology and opto-mechatronic systems.

Mr. Wakana is a Member of the Institute of Electronics, Information and Communication Engineers of Japan, the Japan Society of Applied Physics, and the Optical Society of America.

Etsushi Yamazaki was born in Toyama, Japan. He received the B.E. and M.E. degrees in electronic engineering from the University of Tokyo, Japan, in 2000 and 2002, respectively.

He is currently with NTT Network Innovation Laboratories, Yokosuka, Japan, where he is engaged in research on photonic transport and processing techniques.

Mr. Yamazaki is a member of the Institute of Electronics, Information and Communication Engineers of Japan.

Shunsuke Mitani was born in Kagawa, Japan. He received the B.E. degree in industrial chemistry from Kyoto University, Japan, in 2002. He is currently pursuing the M.E. degree in electronic engineering from the University of Tokyo, Japan.

Mr. Mitani is a member of the Institute of Electronics, Information and Communication Engineers of Japan.

Hyonde Park was born in Fukuoka, Japan, on November 3, 1979. He received the B.E. degree in electronic engineering from the University of Tokyo, Japan, in 2002.

Mizuki Iwanami was born in Tochigi, Japan, in 1968. He received the B.E. degree in materials science and engineering from Waseda University, Tokyo, Japan, in 1991 and the M.E. and Ph.D. degrees in materials science from the University of Tokyo, Tokyo, in 1994 and 1997, respectively.

In 1997, he joined NEC Corporation, Kawasaki, Japan, where he was involved in research on EMI reduction techniques for printed circuit boards. In 2000, he joined the Association of Super-Advanced Electronics Technologies, Tsukuba, Japan. He is currently engaged in research of optical near-field probing techniques and their applications to electronic devices.

Dr. Iwanami is a Member of the Institute of Electronics, Information and Communication Engineers of Japan.

Shigeki Hoshino was born in Fukuoka, Japan. He received the B.E., M.E., and Ph.D. degrees from Kyushu University, Japan, in 1976, 1978, and 1983, respectively, all in physics.

He joined NEC Corporation, Japan, in 1983. In 1999, he joined the Association of Super-Advanced Electronics Technologies, Japan. He has been engaged in research and development of EMI reduction technologies and electromagnetic sensors.

Dr. Hoshino is a Member of the Institute of Electronics, Information and Communication Engineers of Japan and the Japan Society of Applied Physics.

Masato Kishi was born in Tokyo, Japan. He received the B.S. and M.S. degrees in physics from Nihon University, Japan, in 1973 and 1975, respectively.

From 1975 to 1990, he had been with the Institute of Interdisciplinary Research and the Research Center for Advanced Science and Technology, which belonged and belongs to the University of Tokyo, respectively. In 1990, he joined the Department of Electronic Engineering in the same university. He has been involved in research projects in the fields of semiconductor material science and technology as well as in the laboratory education curriculums of the department. His current research interests stay in the advanced characterization techniques for Si and optoelectronic materials with emphases on microscopic Raman spectroscopy and nonlinear optics/optoelectronics.

Masahiro Tsuchiya (M'97) was born in Shizuoka, Japan, on September 28, 1960. He received the B.E., M.E., and Ph.D. degrees, all in electronic engineering, from the University of Tokyo, Japan, in 1983, 1985, and 1988, respectively. His dissertation was on the resonant tunneling phenomena in ultrathin semiconductor heterostructures and related devices.

He was a Postdoctoral Fellow with the University of California at Santa Barbara from 1988 to 1990, and a Research Staff Member with the Research Development Corporation of Japan from 1990 to 1991. In 1991, he joined the Department of Electronic Engineering, University of Tokyo, Tokyo, Japan, as a Lecturer and became an Associate Professor in the same department in 1993. From 1996 to 1997, he spent his sabbatical year as a Visiting Researcher at Bell Laboratories, AT&T / Lucent Technologies, Holmdel, NJ. In 2003, he moved to the Communications Research Laboratory, Koganei, Tokyo. His current research interests remain focused on photonics technologies for ultrafast and high-frequency systems/components, nonlinearity management, and microwave/millimeter-wave systems. He is also interested in advanced optoelectronic materials and implementations of practical optoelectronic systems with those materials.

Dr. Tsuchiya is a Member of the IEEE Lasers & Electro-Optics Society (LEOS), the Japan Society of Applied Physics, and the Institute of Electronics, Information and Communication Engineers (IEICE) of Japan.